

Automated Composite Depth Scale Construction and Estimates of Sediment Core Extension

Lorraine E. Lisiecki

Department of Earth Sciences, Boston University, Boston, Massachusetts, USA

Timothy D. Herbert

Department of Geological Sciences, Brown University, Providence, Rhode Island, USA

A composite section, which reconstructs a continuous stratigraphic record from cores of multiple nearby holes, and its associated composite depth scale are important tools for analyzing sediment recovered from a drilling site. However, the standard technique for creating composite depth scales on drilling cruises does not correct for depth distortion within each core. Additionally, the splicing technique used to create composite sections often results in a 10–15% offset between composite depths and measured drill depths. We present a new automated compositing technique that better aligns stratigraphy across holes, corrects depth offsets, and could be performed aboard ship. By analyzing 618 cores from seven Ocean Drilling Program (ODP) sites, we estimate that $\sim 80\%$ of the depth offset in traditional composite depth scales results from core extension during drilling and extraction. Average rates of extension are $12.4 \pm 1.5\%$ for calcareous and siliceous cores from ODP Leg 138 and $8.1 \pm 1.1\%$ for calcareous and clay-rich cores from ODP Leg 154. Also, average extension decreases as a function of depth in the sediment column, suggesting that elastic rebound is not the dominant extension mechanism.

1. Introduction

Pelagic marine sediments provide many opportunities to recover long, largely continuous paleoclimate records. In situ, this stratigraphy is affected by changes in accumulation rates, bioturbation, compression from depositional overburden, hiatuses, and sea floor disturbances; however, stratigraphic discontinuity can often be minimized by careful drill site selection. Sediment recovery introduces additional sources of uncertainty in the continuity and depth scale of marine stratigraphy. Scientific coring operations often retrieve sediment in successive meter-scale cores, which can result in portions of the sediment record being missed or repeated between each core. To compensate for this problem, multiple holes are often drilled at each site, so that material missed in one hole can be obtained from another.

A composite depth section reconstructs a continuous record of the sediment at a drilling site by splicing together cores from proximal holes. Its corresponding composite depth scale describes the correlation of sediments between holes. Both are important tools for analyzing the sediment recovered from a drilling site. The standard splicing technique for creating composite depth sections [e.g., *Hagelberg et al.*, 1992] has been highly successful with the exception of two notable shortcomings. First, it does not correct for distortion within cores so that a sedimentary feature may have a slightly different composite depth in each hole (e.g., Figure 1). Second, the splicing technique typically results in composite depths which are 10–15% greater than recorded drill depths. Possible causes for this accumulation in depth offset include core extension, duplicate stratigraphy in the composite section, and human bias [*MacKillop et al.*, 1995].

This paper begins by describing previous compositing techniques and estimates of core deformation. Next, we present a new automated compositing technique, which produces high-resolution alignments between holes and corrects

composite depths based on measured drill depths. We compare the performance and labor investment of the new technique to the standard one for seven drilling sites from two Ocean Drilling Program (ODP) legs which recovered different sediment types. Finally, we estimate average core extension and gap sizes from these sites and quantify the effects of previously proposed sources of composite depth offset.

2. Background

Deep Sea Drilling Project (DSDP) Leg 68 [*Prell et al.*, 1982] was the first to drill overlapping holes using the hydraulic piston corer (HPC) and to examine the completeness of stratigraphic recovery. Sites 502 and 503 from that leg were used to construct the first composite sections [*Gardner*, 1982; *Kent and Spariosu*, 1982]. Composite sections of ~ 9.6 -m cores from DSDP Leg 94 were developed using visual core color, CaCO_3 content, and magnetic data [*Ruddiman et al.*, 1989; *Raymo et al.*, 1989]. *Ruddiman et al.* [1987] presented a detailed discussion of the factors governing core depth offsets, percent recovery, coring gaps, and drilling disturbances. Based on observations from Legs 81 [*Roberts et al.*, 1984] and 94, they proposed that sediments with higher water content may be more susceptible to coring disturbances. Composite section development for ODP Site 677 revealed coring gaps of 1–2 m and a 10% growth in composite depths relative to shipboard depth measurements [*Alexandrovitch and Hays*, 1989; *Shackleton et al.*, 1990]. Since that time, 1–2-m coring gaps and composite depth growth have been noted at many other ODP sites [e.g., *Froelich et al.*, 1991; *deMenocal et al.*, 1991; *Murray and Prell*, 1991; *Farrell and Janecek*, 1991; *Hagelberg et al.*, 1992; *Curry et al.*, 1995].

Leg 138 was the first to develop composite depth sections at sea so that drilling recovery could be monitored in real time. *Hagelberg et al.* [1992] describe a standardized technique in which continuously sampled lithologic characteristics, such as color reflectance, magnetic susceptibility, and gamma-ray attenuation, from nearby holes are aligned by

defining a single offset for each core relative to meters below sea floor (mbsf). For the sake of speed and simplicity, the depth scale within cores is not stretched or compressed to align individual stratigraphic features. This technique has been used successfully on ODP cruises for over a decade. Usually holes are within 50 m, although in places with laterally invariant stratigraphy, the technique can align cores from sites several kilometers apart [e.g., *Shackleton et al.*, 1999].

Hagelberg et al. [1992] describe several deficiencies of their technique, similar to discrepancies observed in previous composite depth scales. First, composite depths (mcd) consistently exceed drilling depths measured in mbsf by at least 10%. Some depth inflation is expected due to elastic rebound, but its magnitude suggests that either the drilling process generates additional core extension [e.g., *Lyle et al.*, 1992] or that composite sections do not accurately reproduce in situ stratigraphy [e.g., *MacKillop et al.*, 1995]. Vertical motion of the ship during drilling can create gaps between sections, but material should be missed as often as duplicated, creating no accumulation in offset between mbsf and mcd [*Ruddiman et al.*, 1987]. Lateral drift of the ship relative to the drilling hole can create systematic errors in the measurement of mbsf at a given site but should not exceed 1 m. Tidal heave can also produce systematic depth offsets but cannot explain why composite depth offsets are consistently positive.

In a study of cores from Leg 138, *MacKillop et al.* [1995] estimated the amount of core extension produced by elastic rebound due to removal of sedimentary overburden. They determined that elastic rebound accounts for approximately one-third of the accumulation in composite depth offset. Because signal features in the mbsf scale occur both above and below their corresponding features in the downhole log and exhibit no trend in offset with depth, *MacKillop et al.* [1995] proposed that the Leg 138 composite sections contain an average of 25 cm of duplicate material between each 9.5-m core. The standard technique for APC coring presents one possible source for this duplicate stratigraphy. For each advanced hydraulic piston corer (APC) core, a 9.8-m core sample chamber is fully extended into the bottom of the hole, but the drill string is only advanced 9.5 m between cores. This can produce a 0.3 m overlap between cores containing either a void, duplicate stratigraphy, or sediment dislodged from the hole wall, depending on drill string motion and the stability of the hole [*MacKillop et al.*, 1995]. In contrast, a study of elastic rebound for sediments from Leg 154 attributes 90–95% of depth inflation to sediment rebound [*Moran*, 1997], suggesting the presence of little or no duplicate stratigraphy in those composite sections.

Core properties, such as gamma-ray attenuation porosity evaluator (GRAPE) density measurements, are sometimes aligned to downhole log measurements to reduce large-scale depth distortion in the composite section [e.g., *Lyle et al.*, 1992; *Harris et al.*, 1995]. However, downhole logs are often not available for the upper ~100 mbsf and may have significantly lower resolution than core data. Additionally, adjusting the final composite depth may disguise errors in the composite section because downhole logs often lack the resolution to identify duplicate stratigraphy on scales of less than ~1 m [*Harris et al.*, 1995].

The traditional technique for producing composite depth scales [*Hagelberg et al.*, 1992] makes no correction for depth distortion within each core, which can result in different composite depths for a single stratigraphic feature from different holes (e.g., Figure 1). This becomes a significant problem when samples taken from different offset holes cannot be compared directly using the composite depth scale. For example, a 10-cm offset in alignment could result in

glacial material from one hole being mistakenly identified as interglacial based on $\delta^{18}\text{O}$ stratigraphy from another hole. Misalignments indicate that drilling disturbances often occur within cores, increasing distortion in both the mbsf and mcd depth scales. Disturbances at core tops and bottoms are also suggested by the anomalously low wet-bulk densities frequently found there [*Hagelberg et al.*, 1995].

Post-cruise research often produces a revised composite depth scale (rmcd) using high-resolution alignments of GRAPE, magnetic susceptibility and/or reflectance between holes [e.g., *Hagelberg et al.*, 1995; *Dickens et al.*, 1995; *King and Ellis*, 1997; *Palike et al.*, 2005; *Westerhold and Rohl*, 2006]. This allows for comparison of samples between holes and even the construction of stacks (averages) of core measurements across holes [e.g., *Hagelberg et al.*, 1995; *King and Ellis*, 1997; *Palike et al.*, 2005]. High resolution alignments can also be used to study sedimentation rate variability and core deformation. Given their many uses, producing these alignments aboard ship would be very beneficial.

Several studies [e.g., *Hagelberg et al.*, 1995; *Palike et al.*, 2005] have used the automated inverse correlation technique of *Martinson et al.*, [1982] to produce high-resolution alignments, but this technique has several shortcomings. First, it can only be used to match individual cores to a previously constructed composite section because it is not designed to handle core gaps. Second, the algorithm only finds the locally optimal alignment of cores and is therefore dependent upon a user-defined first guess. Users must also iteratively and subjectively determine the optimal number of coefficients for each mapping function to generate reasonable sedimentation rates. In Section 4.6, we use the rmcd scale of Leg 138 [*Hagelberg et al.*, 1995] to compare the results of our alignment technique with that of *Martinson et al.* [1982].

Alternatively, some rmcd scales [e.g., *Dickens et al.*, 1995; *King and Ellis*, 1997] are produced by manually defining tie points between holes. This procedure can be extremely labor intensive with an alignment resolution proportional to the number of tie points. To produce a composite section for ODP Sites 885/886, *Dickens et al.* [1995] stretched or compressed cores as necessary to align peaks in magnetic susceptibility. With an average tie point spacing of 0.6 m, this strategy was sufficient to align most polarity chron boundaries, biostratigraphic events, and bulk chemistry measurements to within 0.4 mcd. This alignment produced gaps of 0.10–2.85 m and overlaps of 0.10–3.60 m across core breaks. However, the alignments also revealed several instances in which stratigraphy within cores (i.e., not at core breaks) could not be matched across holes. The authors attributed these interhole discrepancies to localized hiatuses and one puzzling instance of “extra” sediment. Interestingly, their composite section does not exhibit an increase in depth relative to mbsf.

3. Method

Our automated compositing technique consists of four basic steps (see Figure 2). First, the sediment from each hole is correlated with the sediment of a selected, “target” hole using the cores’ lithologic characteristics (e.g. reflectance, magnetic susceptibility, and GRAPE density). An automated graphic correlation program modified from *Lisiecki and Lisiecki* [2002; hereafter, referred to as LL02] performs these correlations, correcting for core deformation and estimating core gap sizes. Second, an automated compositing program constructs a continuous composite section by splicing together segments from each hole to avoid gaps and sediment that is likely to be highly deformed. This generates a composite depth scale (mcd) in the same manner as

the traditional technique. Third, a polynomial offset correction is applied to the mcd scale to improve agreement with core top mbsf measurements. Finally, the graphic correlation software aligns each hole to the new composite section to create a conversion from mbsf to corrected mcd (cmcd). Appendix A provides detailed methodology, and Appendix B describes technical modifications to the LL02 algorithm. Source code for all steps is available (supplemental material and <http://lorraine-lisiecki.com>).

4. Results

4.1. Study Sites

The new compositing technique was applied to data from Sites 846, 849, and 851 of ODP Leg 138, which primarily recovered alternating layers of nannofossil and diatom ooze with relatively little clay [Mayer *et al.*, 1992], and Sites 925, 926, 927, and 929 of ODP Leg 154, which primarily recovered calcareous ooze and chalk with significant but variable clay content and little silica [Curry *et al.*, 1995]. The lengths of our composite sections are determined by the maximum depth spanned by at least two holes with good recovery rates. For our seven study sites, the composite sections extend to cmcd depths of 247 m, 330 m, 316 m, 354 m, 380 m, 270 m, and 156 m, respectively. The alignment for these composites was performed primarily using core reflectance because it typically shows the most coherent variability. Alignments for Sites 927 and 929 used both reflectance and magnetic susceptibility data due to weaker reflectance correlations. Our composite sections for each site and mappings from mbsf to cmcd for each hole are provided (supplemental material).

4.2. Tie Points

Because stratigraphic features can vary somewhat between holes and because gap sizes are poorly constrained, some manual correction to the automated alignment by the addition of tie points is often necessary. We added tie points wherever misalignments of more than ~ 0.3 m were observed in the automated alignment, most typically near core breaks. The average number of manually defined tie points in our interhole alignments is 2.5 tie points per core. This translates to approximately 46.6 tie points per 100 m (mbsf) of composite section constructed. Using multiple physical properties for alignments can further reduce the number of tie points required. Sites 927 and 929, which were aligned using reflectance and magnetic susceptibility, required an average of only 2.0 tie points per core (44.0 per 100 m).

In comparison, the traditional construction of composite section requires one tie point per core for each hole, which averages 29.1 tie points per 100 m (mbsf) for our seven study sites (32.3 per 100 m for Sites 927 and 929). Using multiple physical properties and our automated alignment technique, a modest 30–40% increase in tie points can produce high-resolution alignments between holes. Because the algorithm's run time for interhole alignments is only a few minutes, it should be possible to use our alignment and compositing technique aboard ship, thus eliminating the need to create revised composite depth scales during post-cruise research.

4.3. Alignment Evaluation

We compare the performance of our new cmcd scales to the original mcd scales [Mayer *et al.*, 1992; Curry *et al.*, 1995] by finding the correlation coefficient of reflectance versus composite depth across holes. The new technique increases the interhole correlation of reflectance from 0.69 to 0.77 for the three sites from ODP Leg 138 and from 0.70 to

0.80 for the four sites from ODP Leg 154. The performance of our alignment technique appears similar to that of mcd scale for Leg 138 [Hagelberg *et al.*, 1995], which produced an average reflectance correlation of 0.78 between holes at Sites 846, 849, and 851. Increases in interhole correlation translate into a significant improvement in the usefulness of the new composite depth scale by allowing high resolution measurements from different holes to be compared without additional alignment (e.g., Figure 1).

4.4. Core Extension

We estimate average rates of extension and patterns of extension versus depth in core using all 618 cores from Sites 846, 849, 851, 925, 926, 927, and 929 that fall in the depth range of our composite sections. On average, the drilling and recovery process extended the length of the calcareous/siliceous sediment cores from Leg 138 by $12.4 \pm 1.5\%$ (two standard errors) and the calcareous/clay sediment cores of Leg 154 by $8.1 \pm 1.1\%$, as measured by the ratio of recovered core length to length in the new composite section. However, extension rates vary greatly among cores with standard deviations of 11.7% for Leg 138 and 10.4% for Leg 154.

Average extension in Leg 138 cores is more than twice the elastic rebound of 4–5% estimated from sediment consolidation experiments for Sites 844–847 [MacKillop *et al.*, 1995]. However, we observe approximately the same extension in Leg 154 cores as estimated from measurements of elastic rebound at ~ 48 mbsf at Site 929 [Moran, 1997]. Whether the observed extension of these cores is in fact consistent with the process of elastic rebound is discussed in Section 5.2.

Extension as a function of depth in each ~ 9.5 -m core is estimated as the percent increase in the length of each 0.25-m interval between the mbsf and cmcd depth scales. These estimates are undoubtedly affected by the fact that extension is measured relative to composite depth (cmcd), which has not been corrected for small-scale variations in extension. However, averaging across many cores compensates for this source of uncertainty. Figure 3 shows the mean and median of extension versus within-core depth for three types of cores from each leg. Figure 4 shows the distribution of extension rates among all cores of each type.

Average patterns of extension appear to vary as a function of depth in the sediment column and possibly coring device. In most APC cores (those below ~ 50 mbsf), extension is 0% at the core top, $\sim 15\%$ at 1–2 m below the core top, $\sim 10\%$ at 3–7 m, and 0–5% at 8–9 m. However, in the top 6 APC cores of each hole, extension maxima tend to occur near the middle of the core. This difference may be due to higher water content in these cores [Ruddiman *et al.*, 1987; Hagelberg *et al.*, 1995]. Extension in extended core barrel (XCB) cores differs between the two legs. XCB cores from Leg 138 look similar to the deeper APC cores whereas XCB cores from Leg 154 show little to no extension except in the last 1–2 m. Although many cores appear to share a common pattern of extension, variability is quite high, probably due to differences in drilling conditions (e.g., ship heave) and sediment properties as well as measurement uncertainty. The standard deviations of extension is $\sim 15\%$ near the core middle and increases to $\sim 25\%$ near the core top and bottom, where drilling disturbances are more frequently observed.

4.5. Gap Lengths

The new cmcd depth scale should provide an accurate description of the lengths of stratigraphy missing between core breaks. Figure 5 shows the distribution of gap lengths

from each ODP leg in the mbsf scale, the original composite depth scale (mcd), and the new cmcd scale. Gap lengths in mbsf are measured as the difference between the recovered core length and the 9.5-m change in drill depth between core tops. A negative mbsf gap indicates that a recovered core is longer than the depth advanced between core tops and does not necessarily imply that duplicate stratigraphy was recovered (due to depth scale uncertainty and core extension). In contrast, gap lengths in mcd reflect the length of stratigraphy missing between core breaks because the mcd scale aligns cores to the continuous stratigraphy of a composite section. Negative mcd gaps explicitly denote stratigraphic duplication due to coring overlap. Gap lengths in cmcd are calculated in the same way as mcd gap lengths except that gaps are measured relative to a composite section that has been corrected for core extension. Therefore, in Figure 5 mcd gap lengths are reduced by the average rate of core extension on each leg for better comparison with cmcd gap lengths. Correcting for core extension also provides a more accurate estimate of the in situ length of missing stratigraphy.

The distribution of mbsf gap lengths for both legs has a mode of 0 m, a mean of 0.2 m, and a standard deviation of 0.7 m. The percentage of core breaks with negative mbsf lengths is 26% on Leg 138 and 19% on Leg 154. In the original mcd scale, 1.6% and 3.8% of gaps are negative (coring overlaps) for the two legs respectively, and average gap lengths (for gaps smaller than 4 m) are 1.5 m and 1.2 m. When the original mcd gap lengths are scaled down to account for core extension (as in Figure 5), the average mcd gap lengths for the two legs are 1.3 m and 1.1 m. In the cmcd depth scale, 9.5% and 12% of gaps are negative and average gap lengths are 1.1 m and 0.9 m for Legs 138 and 154, respectively.

The difference in average gap length between the mbsf and cmcd depth scales is consistent with our estimates of core extension. “Full-length,” 9.5-m cores may often be associated with the recovery of ~ 8.7 m of in situ stratigraphy that has undergone 8–12% extension. This would produce a gap length of 0 m in mbsf but would correspond to ~ 0.8 m of unrecovered stratigraphy at each core break, consistent with the prevalence of that gap size in the cmcd scale.

4.6. Sensitivity Tests

Sensitivity tests (Figure 6) demonstrate that our estimates of mean gap length and core extension are relatively insensitive to the parameter values used in our alignments (see Appendix B). For these tests, we vary one parameter at a time during the alignment of one hole (849B) to its composite section. This hole contains 37 cores spanning 347 m, and its alignment to the composite section uses 13 manually defined tie points. We test a large range of values for each penalty parameter (see the caption of Figure 6) to compensate for the fact that only one parameter is varied at a time. Decreasing the interval size used by the alignment improves the algorithm’s performance at the expense of greater run times. Decreasing penalty weightings tends to produce a better correlation between records by allowing relative extension rates to vary more. However, if penalty weightings are too low, the algorithm may align the noise in the two records, producing erroneous estimates of core extension.

The average gap length in the alignment is most affected by the “gap-size” penalty, with a factor of 20 change in penalty weighting producing mean gap lengths of 1.33–1.48 m with standard deviations of 0.95–1.26 m. For comparison, the mean gap length of Hole 849B in the mbsf depth scale is 0.48 m. Because the mean mbsf gap length is well

outside of the range of mean cmcd gap lengths produced by different penalty values, we conclude that the mbsf depth scale significantly underestimates the length of stratigraphy missing between cores.

The sensitivity of our extension estimate varies as a function of depth in core because fewer alignment constraints are available near core breaks. Mean extension near the middle of cores varies by $\sim 2\%$ for different penalty weightings, but mean extension for the top and bottom 2 m of each core varies by $\sim 5\%$. The standard deviation of extension is also larger and more sensitive to parameter values near core ends. In the top 2 m of cores, the standard deviation is most affected by the “speed-change” penalty and varies from 15.6–29.2%. Near core middles, it is most affected by the “speed” penalty and varies from 10.1–16.6%.

Comparison of relative extension rates generated by the cmcd and rmcd [Hagelberg *et al.*, 1995] depth scales for Leg 138 provides another check on the sensitivity of our results because the two depth scales are generated using two different automated alignment techniques. When sampled at a scale of 25 cm, the standard deviation of relative extension rates in the rmcd scale is 20–40% for Sites 846, 849, and 851 (Figure 7), slightly larger than the 15–30% observed in our cmcd alignments. The fact that both techniques show greater variability in extension near core tops and ends suggests that this feature is due to actual variability in core deformation rather than an artifact of the alignment algorithm.

Although the cmcd and rmcd alignments produce similar standard deviations for extension as a function of depth in core, the average standard deviation of extension within each 9.5-m core on the rmcd scale (19%) is nearly twice that of cores on the cmcd scale (10%). However, the rmcd scale produces only a slight improvement in the correlation of reflectance between holes (0.78 compared to 0.77 on the cmcd scale). Greater extension variability in the rmcd scale may be an artifact of the sinusoidal mapping functions of the Martinson *et al.* [1982] technique or the number of Fourier coefficients (as many as 47) used by Hagelberg *et al.* [1995]. Our alignment technique produces more conservative estimates of both extension and implied sedimentation rate variability due to drilling disturbances.

5. Discussion

5.1. Sources of Composite Depth Inflation

The compositing technique of Hagelberg *et al.* [1992] inflated composite depths by 15.5% and 10.1% relative to mbsf for the studied sites in Legs 138 and 154, respectively. In Table 1 we estimate the contributions of extension, duplicate material, and bias to the depth inflation of the original mcd scales. In Section 4.4, we estimate the rates of core extension to be 12.4% and 8.1% for the two legs respectively. Elastic rebound presumably contributes to this extension, but other mechanisms may also produce core extension during drilling.

MacKillop *et al.* [1995] proposed that a large fraction of mcd depth inflation in Leg 138 resulted from the inclusion of about 25 cm of duplicate stratigraphy between each core break in the composite. Specific comparison of the splices between the original and new composite sections suggests that splicing errors in the original composite sections account for mcd offsets of 3.9% and 1.3% for Legs 138 and 154, respectively. In particular, we find a large concentration of splicing errors in the original composite section for Site 851 below 150 mbsf, where only two holes are available from which to construct the composite. Between 150–317 mbsf, the original mcd scale is inflated by 26% relative to mbsf, and we estimate that 14.6% of the original composite

section represents duplicate stratigraphy. If this particularly erroneous interval is excluded, average mcd depth inflation for our Leg 138 sites is 14.0%, average core extension is 12.8%, and splicing errors produce mcd offsets of 2.0%.

Human bias, such as preferentially including cores which are the most or least extended in the composite section, presents another possible source of discrepancy between the mcd and mbsf depth scales. However, core extension and previous splicing errors together account for most of the observed depth inflation in the original mcd scale. The remaining differences between original mcd offsets and the estimated contributions of extension and splicing errors are quite small (-0.8% and 0.7% for Legs 138 and 154, respectively) and likely reflect the uncertainty in our estimates. In summary, we find that approximately 80% of the difference between mbsf and original mcd depth scales is due to core extension and that the remaining ~20% is most likely due to the inclusion of duplicate material in the original composite sections.

5.2. Sediment Properties and Extension

Because the physical properties of sediments have been shown to affect elastic rebound [e.g., *MacKillop et al.*, 1995], we now analyze the effects of sediment composition and density on core deformation. The calcareous and siliceous sediments from Leg 138 Sites 846, 849, and 851 average 50% more extension than the calcareous, clayey sediments of Leg 154 Sites 925, 926, 927, and 929. We examine the correlation of extension with carbonate content, GRAPE density, water content, and porosity for the seven study sites over three depth ranges (Table 2). Analysis at different depths allows us to consider changes in composition and extension with depth; however, relatively large depth ranges are necessary to minimize the uncertainty in our extension estimates. Other factors that may affect core extension are clay and biogenic silica concentrations, minor sediment components, grain size, ship movement, and drilling operations.

Based on all 20 extension estimates in Table 2, the correlations between each property and extension are 0.49 for carbonate content, -0.58 for GRAPE, 0.59 for porosity, and 0.70 for water content. We additionally consider property correlations within each of the three depth ranges. The averages of these three depth-specific correlations are 0.61 for carbonate content, -0.60 for GRAPE, 0.66 for porosity, and 0.65 for water content. Based on both calculations, porosity and water content, which are closely related to one another, appear to be slightly better predictors of extension than carbonate content or GRAPE density. For example, Site 925 has the least extension of the four Leg 154 sites from 0–50 m and the most extension from 50–150 m. The same change in the relative ranking of Site 925 is observed in water content and porosity but not in carbonate content or GRAPE density. However, calibration problems with the GRAPE instrumentation on Leg 154 [*Curry et al.*, 1995] may have affected these GRAPE measurements, which should strongly correlate with porosity and water content except in siliceous or organic-rich sediments.

The correlation of each physical property with extension is strongest in the 0–50 m range and tends to decrease with depth. The average magnitude of correlation across property type is 0.90 for 0–50 m, 0.63 for 50–150 m, and 0.35 for 150–250 m. This decrease in correlation with depth may reflect an extension mechanism in shallow sediments that is highly sensitive to sediment properties. This additional source of extension in shallow sediments is also suggested by the negative correlation (-0.19) between extension and cmcd depth in Leg 138 cores (Figure 8). This trend is inconsistent

with elastic rebound as the sole source of extension because rebound increases with depth due to removal of a greater sedimentary overburden. The correlation between extension and depth in Leg 154 cores (-0.02) is also inconsistent with the expected trend due to elastic rebound. Higher than expected rates of extension in shallow cores may result from a greater susceptibility to drilling disturbance in sediments with higher water content [*Ruddiman et al.*, 1987].

We suggest that the rates of extension in Legs 138 and 154 can be explained as the combined effects of elastic rebound and drilling-induced core extension that varies as a function of water content/porosity. This concept can be tested by comparing “excess” extension (the difference between core extension and predicted elastic rebound) with the water content and porosity of the sediments. The extension due to elastic rebound, E_r , can be calculated from the physical properties of the sediment using the equation

$$E_r = (1 - n)C_r \log P'_o \quad (1)$$

where n is porosity, C_r is the coefficient of expansion, and P'_o is the effective vertical overburden stress. *MacKillop et al.* [1995] found that C_r (measured experimentally) can be estimated by

$$C_r = 4.0 \exp(0.19e) \quad (2)$$

where e is the void ratio of the sediment. Using the relationship $n = e/(1+e)$, we find that elastic rebound is negatively correlated with porosity (Figure 9a) for the typical porosity range of sediments from Leg 138. However, the effect of porosity on rebound is much smaller than the effect of changes in overburden stress with depth (e.g., Figure 9b).

When we subtract the elastic rebound predicted by equations 1 and 2 from the observed whole-core extension and exclude outliers more than two standard deviations from the mean, we find that excess extension is weakly correlated with porosity (0.40) and water content (0.38) at Site 846 (Figure 9c). Correlations between excess extension and porosity are ~0.33 at the other six study sites. (These correlations are not directly comparable to those for the three depth intervals in Table 2 because these correlations compare individual cores within a single hole whereas those compare extension between sites, averaged over 50–100 m.) Although the correlations between extension and porosity are weak, they cannot be explained by elastic rebound, which predicts a negative correlation. Therefore, an additional mechanism related to the porosity/water content of sediments appears to play a significant role in the extension of APC cores. However, determining the nature of this mechanism is beyond the scope of this study.

5.3. Visual Core Descriptions and Extension

Shipboard visual core descriptions (VCD) include many instances of apparent drilling disturbances. Here we compare the VCD of 327 cores from Sites 846, 849, 925, and 926 [*Mayer et al.*, 1991; *Curry et al.*, 1995] with our estimates of core extension, calculated without reference to the VCD. We focus on anomalously high and low extension rates because no visual evidence exists for the pervasive extension that appears to affect most sediment cores. *Lyle et al.* [1992] suggested that “the coring process may both subtly compress and lengthen the recovered cores, as if the sediment had been squeezed through a die during coring.”

Descriptions of soupy or highly disturbed material are very common in the top 0.1–0.5 m of cores, particularly in

the first 10–20 cores from each hole. This soupy and/or disturbed material at core tops may explain the greater variability of extension near core tops and may be responsible for the pattern of little to no extension in the top ~1 m of cores compared to the 8–15% extension throughout the rest of the core. However, we observe that the low extension rates at core tops often extend deeper than the described disturbance. This discrepancy could easily be an artifact of limitations placed on extension rate changes during alignment, or core tops disturbances could extend 0.5–1 m deeper than visual assessment indicates.

Visual evidence of core extension is rare. The VCD logs describe stretching or flow-in in only 22 of 327 cores. Of four observations of stretching in the VCD, three corresponded to high extension rates on the cmcd scale, and the other was incorporated into the composite section, which may reduce the accuracy of our extension estimate. Of 18 observations of flow-in, 10 corresponded to high extension rates on the cmcd scale, four showed compression, and four showed only minor changes. Unexplained voids also sometimes correspond to intervals of core extension.

Observations of drilling disturbances are quite common in APC and XCB cores below ~200 mbsf at Sites 925 and 926 and often extend throughout the entire core length. In the case of Site 925, VCD reports of “sediment biscuits in a softer matrix” may be a sign of sediment extension because rates of extension at Site 925 increase dramatically with depth (Table 2). However, the same correlation between bicuiting and extension is not observed at Site 926, perhaps because of its lower carbonate concentration.

In ~10% of cores we observe larger than average rates of extension or compression which do not correspond to any disturbances noted in the VCD. In some cases, the signs of disturbance may have been deemed too subtle to mention or may have been difficult to spot due to the absence of sharp bedding contacts. It may also be possible that some drilling disturbances produce anomalous rates of extension or compression without producing any stratigraphic distortion. However, some apparent extension anomalies undoubtedly result from alignment errors or the inclusion of disturbed material in the composite section. Such errors cannot be completely eliminated given the large number of cores which must be aligned, but using the VCD to guide the alignment and splicing process should help minimize them.

References

- Alexandrovich, J.M., and J. D. Hays, (1989), High-resolution stratigraphic correlation of ODP Leg 111 Holes 677A and 677B and DSDP Leg 69 Hole 504. In Becker, K., Sakai, H., et al., *Proc. ODP, Sci. Results, 111*, College Station, TX (Ocean Drilling Program), 263–276.
- Curry, W. B., N. J. Shackleton, C. Richter, and Shipboard Scientific Party (1995), *Proc. Ocean Drill. Program Initial Rep., 154*, College Station, TX (Ocean Drilling Program).
- deMenocal, P., J. Bloemendal, and J. King (1991), A rock-magnetic record of monsoonal dust deposition to the Arabian Sea: evidence for a shift in the mode of deposition at 2.4 Ma. In Prell, W.L., Niitsuma, N., et al., *Proc. ODP, Sci. Results, 117*, College Station, TX (Ocean Drilling Program), 389–407.
- Dickens, G. R., H. Snoeckx, E. Arnold, J. J. Morley, R. M. Owen, D. K. Rea, and L. Ingram (1995), Composite depth scale and stratigraphy for Sites 885/886, *Proc. ODP, Sci. Results, 145*, 205–217.
- Farrell, J.W., and T. R. Janecek (1991), Late Neogene paleoceanography and paleoclimatology of the northeast Indian Ocean (Site 758). In Weissel, J., Peirce, J., Taylor, E., Alt, J., et al., *Proc. ODP, Sci. Results, 121*, College Station, TX (Ocean Drilling Program), 297–358.
- Froelich, P.N., P. N. Malone, D. A. Hodell, P. R. Ciesielski, D. A. Warnke, E. Westall, E. A. Hailwood, D. C. Nobes, J. Fenner, J. Mienert, C. J. Mwenifumbo, and D. W. Muller (1991), Biogenic opal and carbonate accumulation rates in the subantarctic South Atlantic: the late Neogene of Meteor Rise Site 704. In Ciesielski, P.F., Kristoffersen, Y., et al., *Proc. ODP, Sci. Results, 114*, College Station, TX (Ocean Drilling Program), 515–550.
- Gardner, J.V. (1982), High-resolution carbonate and organic-carbon stratigraphies for the late Neogene and Quaternary from the western Caribbean and eastern equatorial Pacific. In Prell, W.L., Gardner, J.V., et al., *Init. Repts. DSDP, 68*, Washington (U.S. Govt. Printing Office), 347–364.
- Hagelberg, T., N. Shackleton, N. Pisias, and Shipboard Scientific Party (1992), Development of composite depth sections for sites 844 through 854, *Proc. ODP, Init. Repts., 138 (Pt. 1)*, 79–85.
- Hagelberg, T. K., N. G. Pisias, N. J. Shackleton, A. C. Mix, and S. Harris (1995), Refinement of a high-resolution continuous sedimentary section for studying equatorial Pacific Ocean paleoceanography, Leg 138, *Proc. ODP, Sci. Results, 138*, 31–46.
- Harris, S., T. Hagelberg, A. Mix, N.G. Pisias, and N.J. Shackleton (1995), Sediment depths determined by comparisons of GRAPE and logging density data during Leg 138, *Proc. ODP, Sci. Results, 138*, 47–57.
- Kent, D.V., and D. J. Spariosu (1982), Magnetostratigraphy of Caribbean Site 502 hydraulic piston cores. In Prell, W.L., Gardner, J.V., et al., *Init. Repts. DSDP, 68*, Washington (U.S. Govt. Printing Office), 419–433.
- King, T. A., and W. G. Ellis, Jr. (1997), Development of a high quality natural gamma data set from Ceara Rise: Critical groundwork for core and log data integration, *Proc. ODP, Sci. Results, 154*, 117–134.

6. Conclusions

We present a new technique for developing composite depth scales which requires only slightly more labor than the traditional technique but significantly improves the correlation of stratigraphic features between holes and keeps composite depths in agreement with mbsf measurements. Approximately 80% of the depth inflation observed in traditional composite sections appears to result from core extension, with the remaining 20% resulting from the inclusion of duplicate stratigraphy in the original composite sections. Rates of extension are highly variable but we find that core extension is often greatest in shallow sediments, perhaps because sediments with greater water content/porosity are more susceptible to extension during coring. Average patterns of extension within cores also vary as a function of depth; cores from the top 60 m tend to be most stretched 3–9 m below the core top while those from deeper than 60 m are often most stretched 1–2 m below the core top. Finally, because extension tends to decrease with depth below the sea floor and is positively correlated with porosity, we conclude that elastic rebound is not the dominant mechanism responsible for core extension.

Acknowledgments.

The authors thank P. Lisiecki for his contribution to modifying the alignment software and also G. Dickens and an anonymous reviewer for their insightful suggestions, which have greatly improved this manuscript. This research used data provided by the Ocean Drilling Program (ODP). The ODP is sponsored by the U.S. National Science Foundation (NSF) and participating countries under the management of Joint Oceanographic Institutions (JOI) Inc. Funding for this research was provided by a Schlanger Ocean Drilling Fellowship, which is part of the NSF-sponsored U.S. Science Support Program (USSSP). Additional support was provided by the NOAA Postdoctoral Program in Climate and Global Change, administered by the University Corporation for Atmospheric Research.

- Lisiecki, L. E., and P. A. Lisiecki (2002), Application of dynamic programming to the correlation of paleoclimate records, *Paleoceanography*, 17, doi:10.1029/2001PA000733.
- Lyle, M., L. Mayer, N. Pisias, T. Hagelburg, K. Dadey, S. Bloomer, Downhole logging as a paleoceanographic tool on ocean drilling program leg 138: Interface between high-resolution stratigraphy and regional syntheses, *Paleoceanography*, 7, 691–700, 10.1029/92PA02073, 1992.
- MacKillop, A. K., K. Moran, K. Jarrett, J. Farrell, and D. Murray (1995), Consolidation properties of Equatorial Pacific Ocean sediments and their relationship to stress history and offsets in the Leg 138 composite depth sections, *Proc. ODP, Sci. Results*, 138, 357–369.
- Martinson, D. G., W. Menke, and P. Stoffa (1982), An inverse approach to signal correlation, *Journal of Geophys. Res.*, 87 B6, 4807–4818.
- Mayer, L. A., N. G. Pisias, T. R. Janecek, and the Shipboard Scientific Party (1991), *Proc. ODP, Init. Repts.*, 138, College Station, TX (Ocean Drilling Program).
- Moran, K. (1997), Elastic property corrections applied to Leg 154 sediment, Ceara Rise, *Proc. ODP, Sci. Results*, 154, 151–155.
- Murray, D.W., and W. L. Prell (1991), Pliocene to Pleistocene variations in calcium carbonate, organic carbon, and opal on the Owen Ridge, northern Arabian Sea. In Prell, W.L., Niitsuma, N., et al., *Proc. ODP, Sci. Results*, 117, College Station, TX (Ocean Drilling Program), 343–363.
- Pälike, H., Moore, T., Backman, J., Raffi, I., Lanci, L., Pars, J.M., and Janecek, T. (2005), Integrated stratigraphic correlation and improved composite depth scales for ODP Sites 1218 and 1219. In Wilson, P.A., Lyle, M., and Firth, J.V. (Eds.), *Proc. ODP, Sci. Results*, 199, 1–41.
- Prell, W.L., Gardner, J.V., et al., (1982) *Init. Repts. DSDP*, 68, Washington (U.S. Govt. Printing Office).
- Raymo, M.E., W. E. Ruddiman, J. Backman, B. M. Clement, and D. G. Martinson, D.G. (1989). Late Pliocene variation in Northern Hemisphere ice sheets and North Atlantic deep water circulation, *Paleoceanography*, 4, 413–446.
- Ruddiman, W. F., Cameron, D., and Clement, B. M. (1987), Sediment disturbance and correlation of offset holes drilled with the hydraulic piston corer: Leg 94, *Init. Repts. DSDP*, 94, 615–634.
- Ruddiman, W. F., M. E. Raymo, D. G. Martinson, B. M. Clement, and J. Backman, J. (1989), Pleistocene evolution: Northern Hemisphere ice sheets and North Atlantic Ocean, *Paleoceanography*, 4, 353–412.
- Shackleton, N. J., A. Berger, and W. R. Peltier (1990), An alternative astronomical calibration of the lower Pleistocene time scale based on ODP Site 677, *Trans. R. Soc. Edinburgh, Earth Sci.*, 81, 251–261.
- Shackleton, N. J., S. J. Crowhurst, G. P. Weedon, and J. Laskar (1999), Astronomical Calibration of Oligocene-Miocene Time, *Philosophical Transactions: Mathematical Physical and Engineering Sciences*, 357, 1907–1929.
- Westerhold, T., and U. Röhl (2006), Data report: Revised composite depth records for Shatsky Rise Sites 1209, 1210, and 1211. In Bralower, T.J., Premoli Silva, I., and Malone, M.J. (Eds.), *Proc. ODP, Sci. Results*, 198, 1–26.

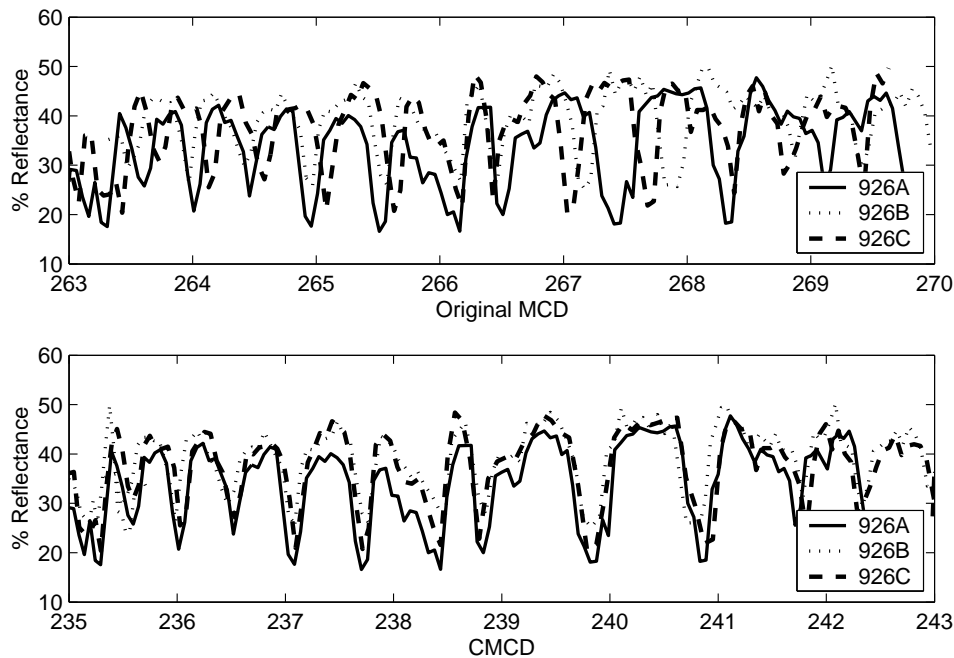
Lorraine E. Lisiecki, Department of Earth Sciences, Boston University,
675 Commonwealth Avenue, Boston, Massachusetts 02215, USA. (lisiecki@bu.edu)

Table 1. Sources of Composite Depth Inflation

	Leg 138	Leg 154
Original mcd inflation	15.5%	10.1%
Core extension	12.4%	8.1%
Original splicing errors	3.9%	1.3%
Potential human bias	-0.8%	0.7%

Table 2. Average Sediment Composition and Extension

ODP Site	846	849	851	925	926	927	929
0–50 m							
Extension (%)	17.1	15.1	17.1	4.2	11.3	7.6	7.0
Carbonate (%)	60	75	79	42	35	35	26
GRAPE	1.35	1.39	1.40	1.66	1.60	1.60	1.55
Porosity (%)	79	78	78	66	68	69	69
Water (% dry wt)	160	140	147	73	77	80	82
50–150 m							
Extension (%)	15.6	16.8	11.4	12.2	7.4	6.8	10.1
Carbonate (%)	49	74	75	63	63	50	41
GRAPE	1.37	1.45	1.46	1.80	1.68	1.70	1.67
Porosity (%)	78	74	75	62	61	61	60
Water (% dry wt)	157	116	121	59	58	55	54
150–250 m							
Extension (%)	9.4	11.6	11.5	14.5	5.6	8.7	N/A
Carbonate (%)	70	73	65	73	63	69	N/A
GRAPE	1.48	1.47	1.44	1.84	1.82	1.79	N/A
Porosity (%)	72	72	75	55	54	55	N/A
Water (% dry wt)	103	102	121	45	43	45	N/A

**Figure 1.** Example of poor alignment in the original mcd scale [Curry *et al.*, 1995] and the same stratigraphic section aligned using our new automated compositing technique.

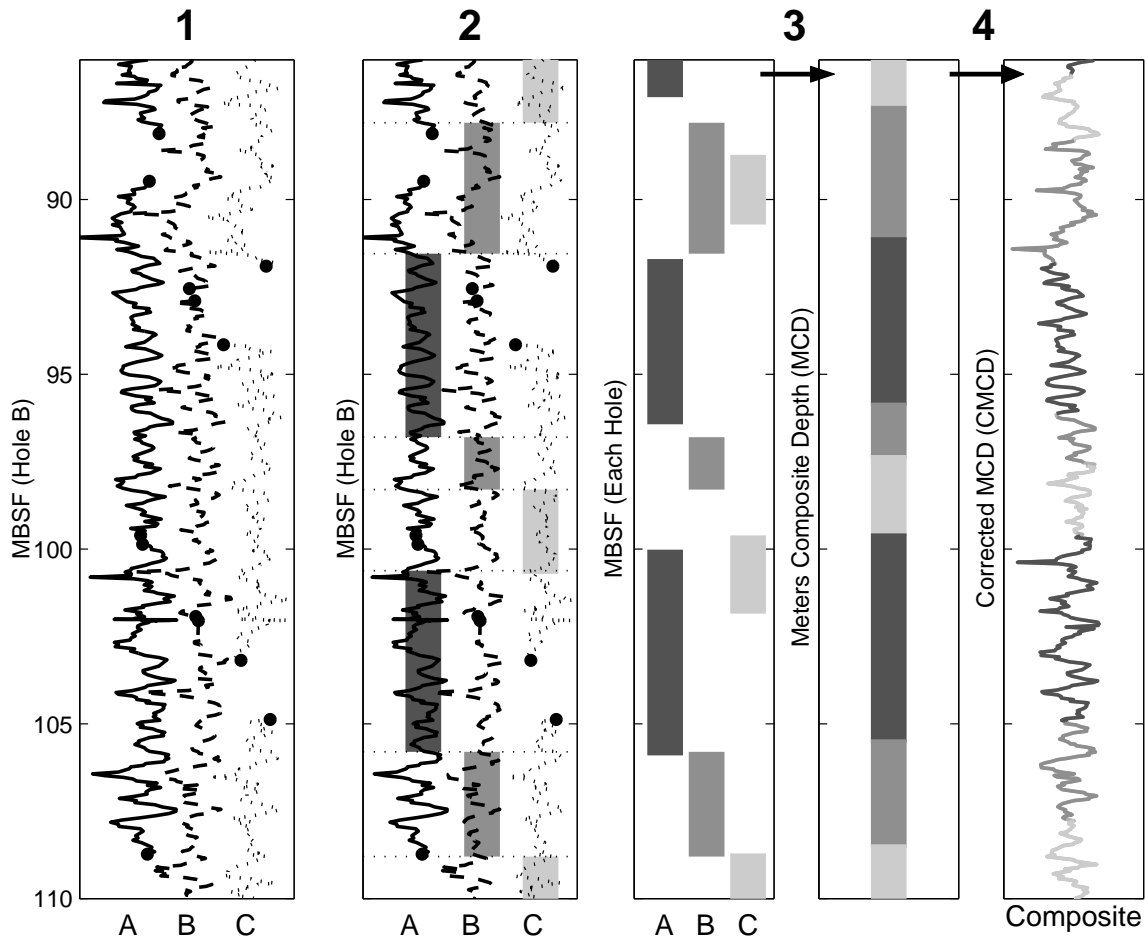


Figure 2. Steps of automated compositing technique. 1) Automated graphic correlation aligns each hole to the target hole. (Dots mark the tops and ends of each ~9.5-m core.) 2) Divide the length of the target into segments from different holes, avoiding core gaps and deformed material where possible. 3) Place segments end-to-end, using their original mbsf scale, to create a the mcd depth scale. 4) Create a corrected mcd (cmcd) depth scale by fitting the mcd of core tops to their mbsf measurements (see text). 5) Align each hole to the composite section (not shown).

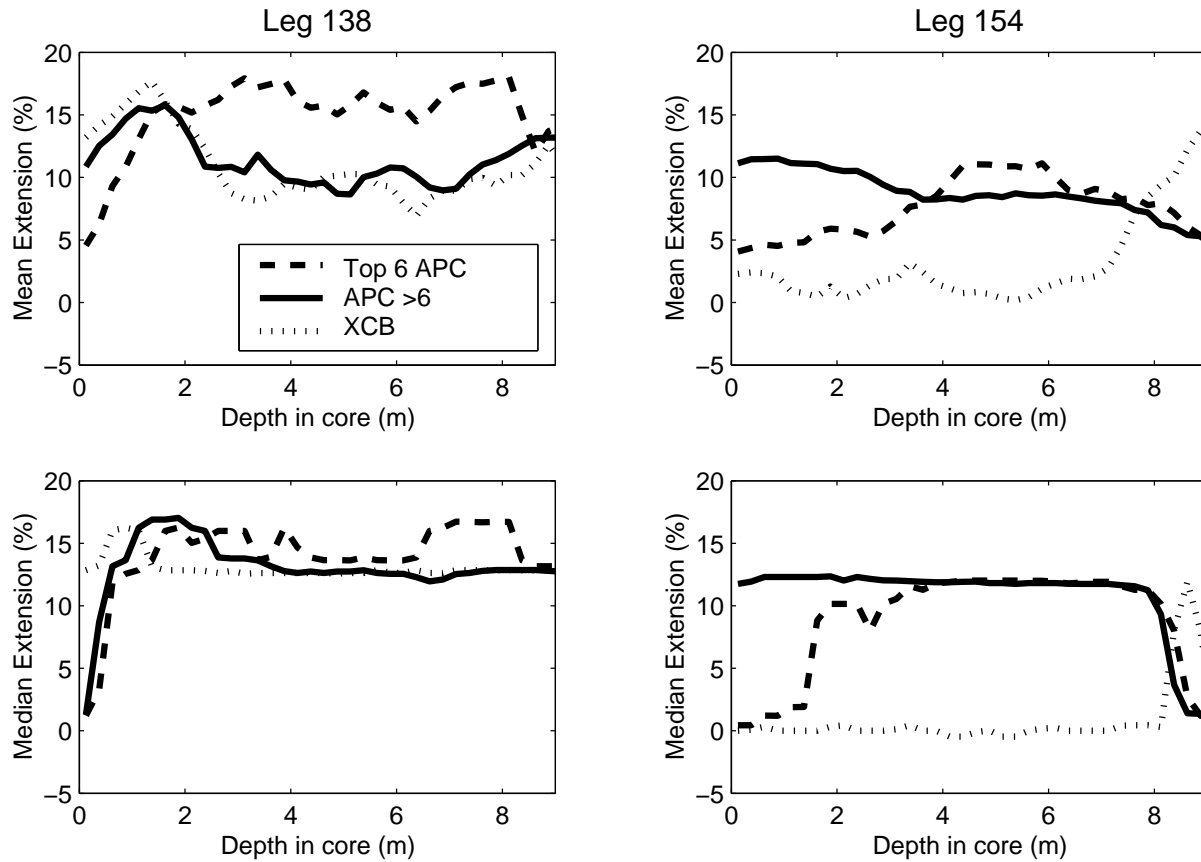


Figure 3. Mean and median of extension by leg and core type for the top 6 APC cores, deeper APC cores, and XCB cores. These are estimated from the following number of cores: 56 upper APC, 83 lower APC, and 96 XCB in Leg 138 and 78 upper APC, 242 lower APC, and 43 XCB in Leg 154.

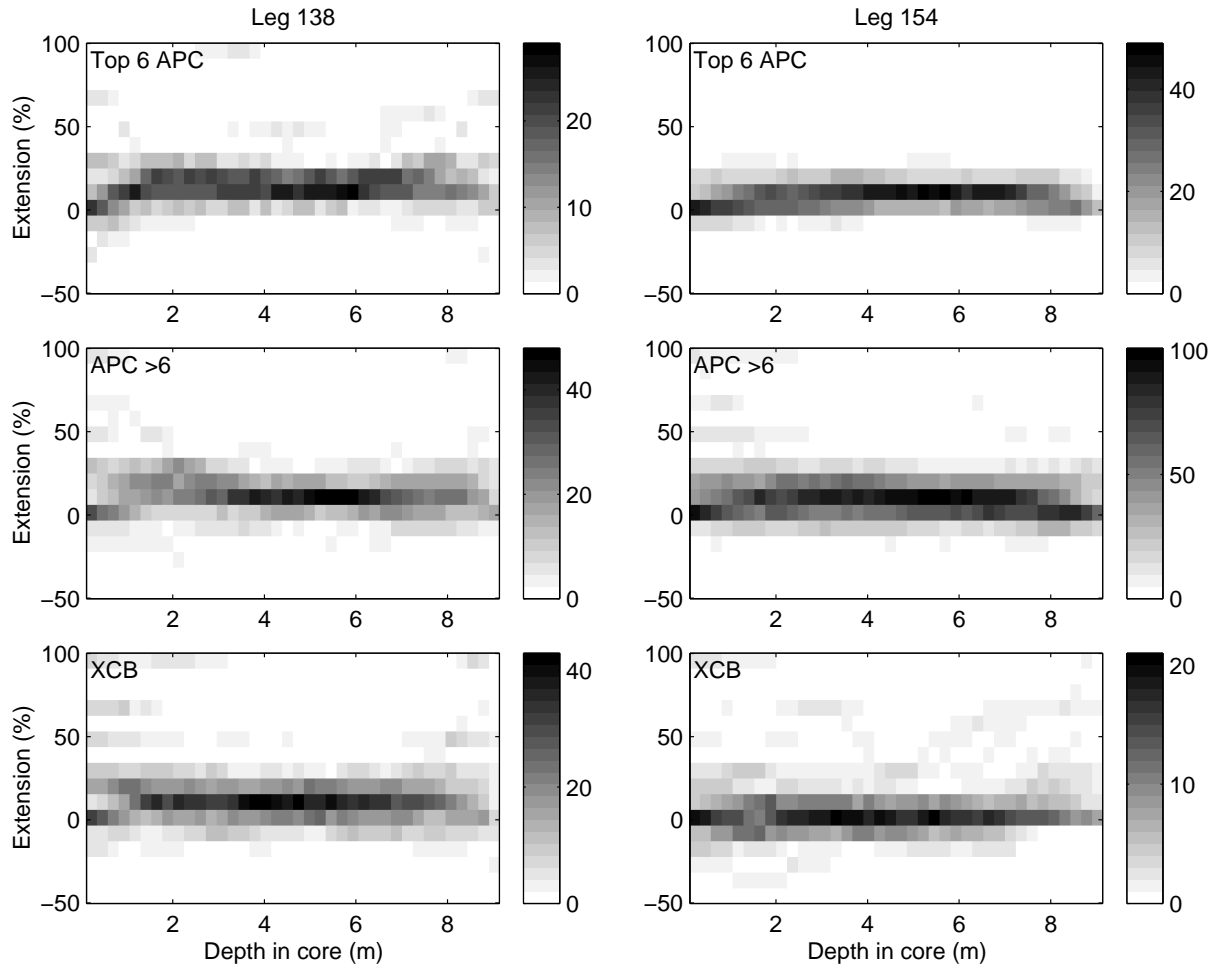


Figure 4. Distribution of extension as a function of depth in core. Grayscale denotes number of cores with a particular extension for each 25-cm interval.

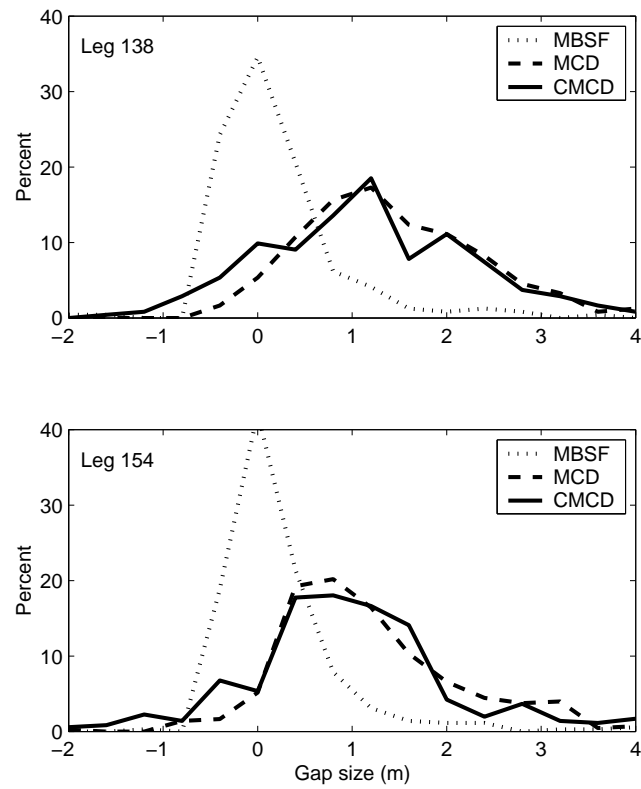


Figure 5. Distribution of gap sizes in the mbsf, original mcd, and cmcd scales. (The mcd sizes have been scaled down by 12.4% and 8.1% to compensate for core expansion in Legs 138 and 154, respectively.)

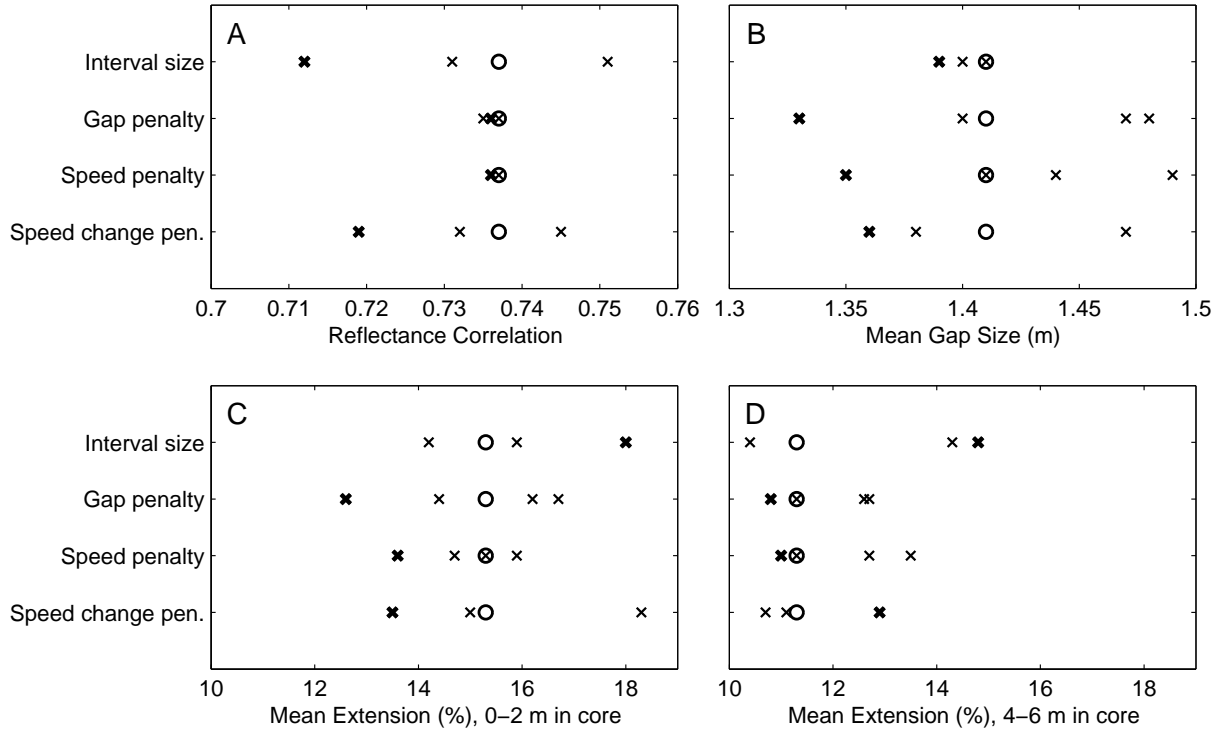


Figure 6. Effect of different parameter values on the alignment of 849B to the composite section: (A) correlation of reflectance in 849B with 849C and 849D, (B) mean gap size in 849B, and (C and D) estimates of mean core extension in 849B from 0–2 m and 4–6 m below the core top. Results are plotted for interval sizes of 15, 25 (default), 35, and 50 cm; for gap penalties of 25, 70, 120 (default), 200, and 500; for speed penalties of 25, 70, 120 (default), 200, and 500; and for speed change penalties of 25, 70 (default), 200, and 500. Circles mark the results for default values, and bold crosses mark the results for the maximum of each parameter value.

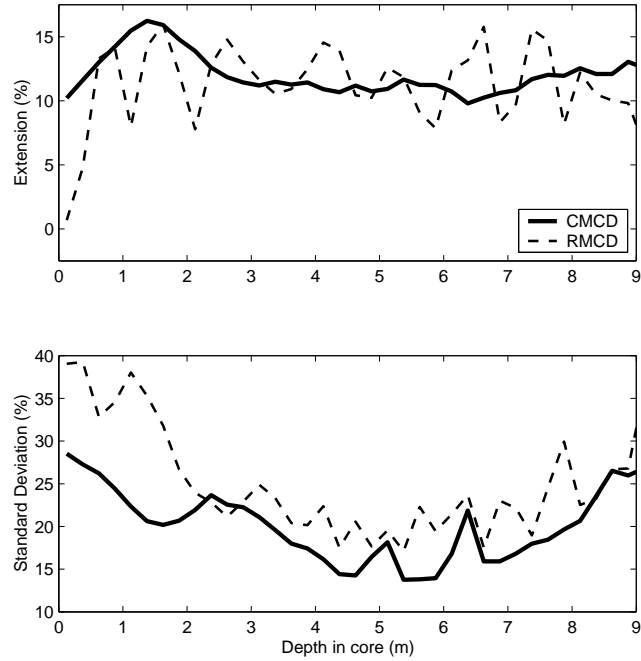


Figure 7. Estimates of extension as a function of depth in core derived from the cmcd and rmcd [Hagelberg *et al.*, 1995] alignments for Sites 846, 849, and 851. A constant offset of 12% has been added to rmcd extension estimates because the rmcd scale aligns cores to the original composite section, which does not correct for average extension rates. Both alignments have similar standard deviations in extension as a function of depth in core.

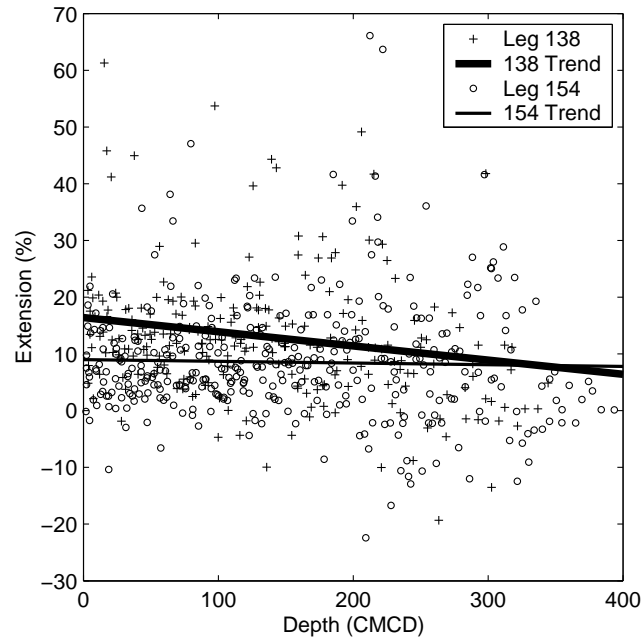


Figure 8. Whole-core extension versus depth in cmcd for Legs 138 and 154. Both show trends of decreasing extension with depth, which is inconsistent with elastic rebound as the primary extension mechanism.

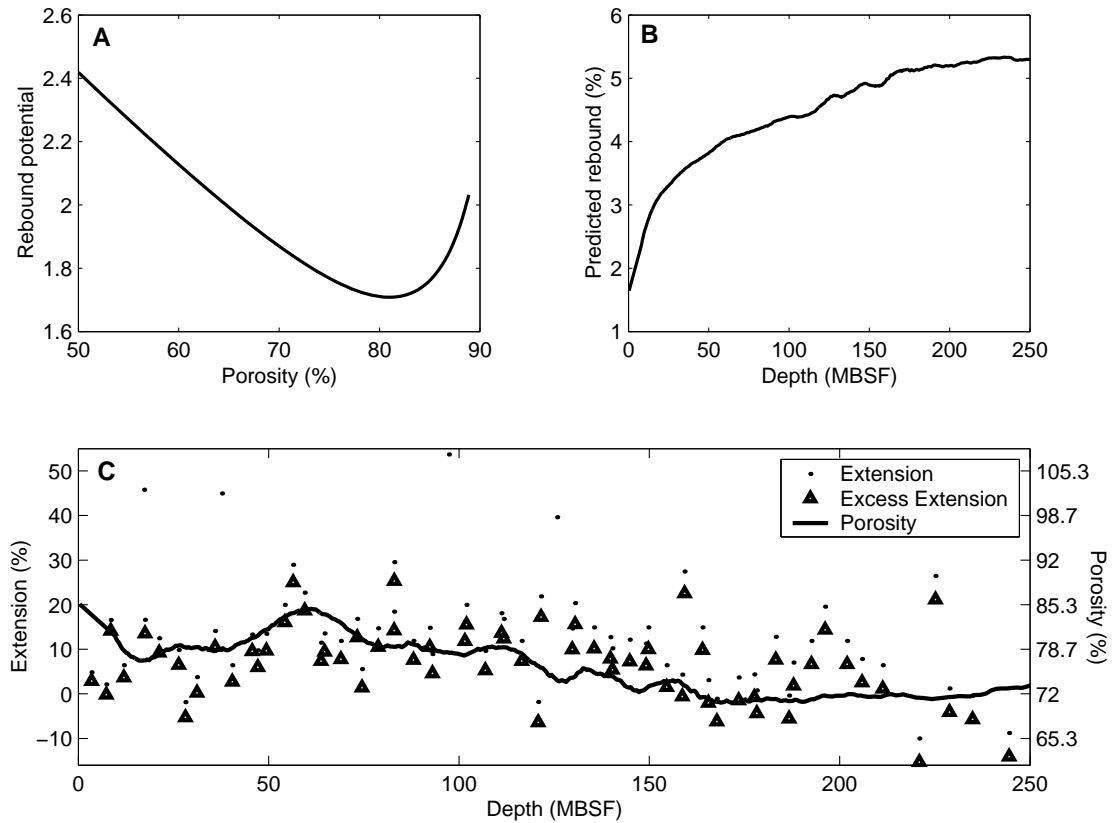


Figure 9. Extension, elastic rebound, and porosity for Site 846. A) Rebound potential $R = C_r(1 - n)$ as a function of porosity n with $n = e/(1 + e)$ and $C_r = 4.0e^{0.19e}$ as empirically derived by *MacKillop et al.* [1995]. B) Predicted rebound, $R \log P'_o$, as a function of depth. C) Whole-core extension and "excess" extension (extension minus predicted rebound) compared to porosity [*Mayer et al.*, 1991] smoothed with a 15-kyr moving window. Outliers excluded from the correlation calculations are plotted for whole-core extension (dots) but not excess extension (triangles).